A Method for Predicting Far Field Radar Cross-section from Near Field Measurements on Cylindrical Scanning Mode

C. Gao[1, 2], J. W. Chen[1, 2], M. Jin[2], and Y. Bai[2]

[1]Information Engineering School, Communication University of China, Beijing 100024, China
[2]Science and Technology on Electromagnetic Scattering Laboratory, Beijing 100854, China

Abstract— For studying the EM signatures of full-size target, it demands outdoor or indoor room large enough for measurement, but the construction of outdoor and indoor room which satisfy the far field conditional both lead to costly installation and require extraordinary elaborate technique, say nothing of carrying out the imaging and RCS diagnostic for stealth weapon in active service. This paper meets the demand of the development with the stealth and anti-stealth weapon, aims at the shortage of outdoor and indoor measuring of the far field electromagnetism feature, presents a research on 3-D near-field to far-field transformation algorithm, in which the far-field condition could not be satisfied on both vertical and horizontal plane for the target under test, and the target is illuminated by a spherical wave. A 3-D multi-scattering center model is built for the target and the near-field data is sampled by 3-D scan, using the extensions of spherical-wave function in cylindrical coordinates, the relationship between far-field and near-field scattering field is deduced under the condition that the antenna works at cylindrical-scan mode. The RCS and image pattern can be achieved by the 3-D IFFT algorithm and interpolation technique. The simulation results show that the algorithm is precise and effective.

1. INTRODUCTION

RCS measurement is necessary for designing stealth weapon system as well as for the research of the electromagnetic scattering properties of radar-illuminate target. The theory and algorithm of electromagnetic scattering computation can be verified by RCS measurement, moreover, it's difficult to compute electromagnetic scattering of complex and large objects, but the data can be obtained visually by RCS measurement.

However, due to the strong frequency-dependent scattering behavior of electromagnetic waves, it is often necessary to conduct the measurements using full-size structures rather than scale-models at high frequencies. Consequently, even moderately large components, as well as larger full-scale structures, have to be measured using outdoor radar measurement ranges. To reduce the cost and time consumed in outdoor range measurement, it is advantageous to develop a capability for characterizing representative structural components that are electrically large within a near distance. This always involves the near-field to far-field RCS measurements transformation methods which is mentioned in [1–5]. The near-field RCS measurement method based on plane scan mode has been presented in [6], while numerical simulation results proves the feasibility and superiority of the method.

But near field to far field transformation based on plane scanning mode is in the rectangular coordinate, in which the near field data grabbing is conducted on the wide plan scan stand, the near field testimony for the electro-magnificent dimension target requires high demand to the aperture and machining decision of the scan stand, however, many microwave anechoic or indoor testing yard could not reach the above criterion because of the confinement of the field. The more widely used near field scatter data collection mode is cylindrical-scan mode (the target rotates, and the radar antenna move along the vertical line to the ground), in order to control the test cost and improve the efficiency.

This paper presents a near field to far field transformation method based on cylindrical scan mode, which utilize the extensions of spherical-wave function in cylindrical coordinates, to deduce the relationship between far-field and near-field scattering field in cylindrical scan mode.

2. NEAR FIELD TO FAR FIELD TRANSFORMATION

The near field cylindrical scan illustration setup is shown in Fig. 1, in which the emit and receive antenna is placed along the vertical track (axis z), move linearly in a fixed step, and the target rotates under the control of the rotate platform in a linearly equal angle interval, antenna measures and records the scatter field data of the target, including the amplitude and phase, on every wave

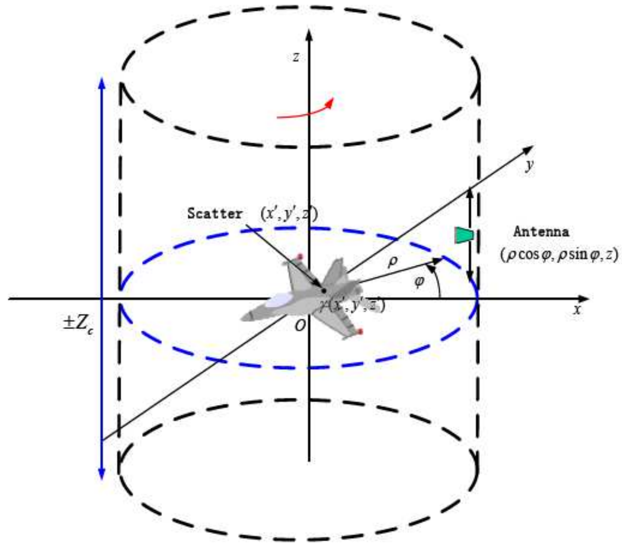

Figure 1: Cylindrical scan mode illustration.

frequency according to the fixed starting frequency and band width, then move to the next record point to repeat.

The time-harmonic weight of the electro-magnetic wave is $e^{-j\omega t}$, the scattering field signal of the target backscatter could be written as:

$$u(k,\varphi,z)=\frac{1}{(4\pi)^2}\iiint\gamma(x',y',z')\left[\frac{e^{-j2kR}}{R^2}\right]dx'dy'dz' \tag{1}$$

where,

$$R=\sqrt{(x'-\rho\cos\varphi)^2+(y'-\rho\sin\varphi)^2+(z'-z)^2} \tag{2}$$

The square brackets in Equation (1) is double-distance spherical factor e^{-j2kR}/R^2, as to the three-dimensional scatter target, the near field illumination is spherical illumination, as to set up the relation between the near field scatter and far field scatter, the double-distance spherical wave factor needs to be transformed into the single-distance spherical factor e^{-j2kR}/R.

According to the character of the Fourier Transform, the realization of the transformation between the double-distance spherical wave factor and the single-distance spherical factor is very convenient when assuming wideband measurements, it just needs to conduct 2 Fourier transform in the frequency domain and distance domain, as follows:

$$U(k,y,z)==\frac{1}{\pi}\int R\left[\int u(k,y,z)e^{-j2kR}dk\right]e^{j2kR}dR \tag{3}$$

The Equation (3) equals to add-up the echo data $u(k,\varphi,z)$ in the distance domain, in which the add-up factor is R, the detailed process is shown in following diagram:

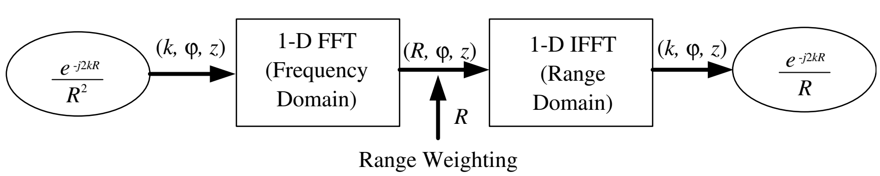

Figure 2: The distance domain add-up process.

Then the Equation (1) transforms into

$$U(k,\varphi,z)=\frac{1}{4\pi}\iiint\gamma(r')\left[\frac{e^{-j2k|\mathbf{r}-\mathbf{r}'|}}{4\pi\,|r-r'|}\right]dr^3 \tag{4}$$

The square brackets in the above equation are spherical wave factor, also called as the free space Green Function, which has the form:

$$\psi = \frac{e^{-j2k|\mathbf{r}-\mathbf{r}'|}}{4\pi\left|\mathbf{r}-\mathbf{r}'\right|} \tag{5}$$

Express ψ with the basic wave function in rectangular coordinate

$$\psi = \iiint\limits_{\kappa_x\kappa_y\kappa_z} A(\kappa_x, \kappa_y, \kappa_z) e^{-j\boldsymbol{\kappa}\cdot\mathbf{r}} d\kappa_x d\kappa_y d\kappa_z \tag{6}$$

In the infinitely large uniform space, the point source field located at the source point $\mathbf{r}'$ satisfies the scalar Hermhoz Equation

$$\nabla^2\psi + k^2\psi = \delta\left(\mathbf{r}-\mathbf{r}'\right) \tag{7}$$

Conduct the plane wave extension of the Green function under the 3-dimensional rectangular coordinate, the Equation (4) changes its form into:

$$\psi = \frac{j}{8\pi^2} \iiint\limits_{k_y k_z} \frac{e^{-j[k_x|x-x'|+k_y(y-y')+k_z(z-z')]}}{k_x} dk_y dk_z$$

In which

$$\begin{cases} k_y = \kappa_y \\ k_z = \kappa_z \\ k_x = \sqrt{k^2 - k_y^2 - k_z^2} \end{cases} \tag{8}$$

Calculated from the above equation, $k_x^2+k_y^2+k_z^2 = k^2$, the factor $k_x(x-x')+k_y(y-y')+k_z(z-z')$ in the Equation (7) denote the plane wave's phase factor, and $j/8\pi^2 k_x$ represents the plane wave amplitude. The integration transform could be utilized to simplify the 3-D integration with 2-D integration, and deduce the spherical factor extension under cylindrical coordinate.

In cylindrical coordinate, the wavenumber and coordinate have the form:

$$\begin{cases} k_x = k_\rho \cos\varphi \\ k_y = k_\rho \sin\varphi \\ x - x' = \rho\cos\varphi' \\ y - y' = \rho\sin\varphi' \\ k_\rho^2 + k_z^2 = k^2 \end{cases} \tag{9}$$

Using the above relation, the Equation (7) transforms into

$$\begin{aligned} \psi &= \frac{j}{8\pi^2} \int_0^\infty \frac{e^{-j\sqrt{k^2-k_\rho^2}(z-z')}}{\sqrt{k^2-k_\rho^2}} k_\rho dk_\rho \int_{-\pi}^{\pi} e^{-jk_\rho\rho\cos(\varphi-\varphi')} d\varphi \\ J_0(x) &= \frac{1}{2\pi} \int_{-\pi}^{\pi} e^{-jx\cos(\varphi-\varphi')} d\varphi \end{aligned} \tag{10}$$

Subscribe into Equation (5), and one gets

$$\psi = \frac{j}{4\pi} \int_0^\infty \frac{J_0\left(k_\rho\rho\right) e^{-j\sqrt{k^2-k_\rho^2}(z-z')}}{\sqrt{k^2-k_\rho^2}} k_\rho dk_\rho \tag{11}$$

Using the relation between the Brussels Function and Hanker Function, the above equation can be expressed as

$$\psi = \frac{j}{8\pi} \int_0^\infty \frac{H_0^2(k_\rho\rho) e^{-j\sqrt{k^2-k_\rho^2}(z-z')}}{\sqrt{k^2-k_\rho^2}} k_\rho dk_\rho \tag{12}$$

Subscribe the Equation (12) into Equation (3)

$$U(k,\varphi,z)=\int\rho(r')\frac{j}{8\pi}\int_0^\infty\frac{H_0^2(k_\rho\rho)e^{-j\sqrt{k^2-k_\rho^2}(z-z')}}{\sqrt{k^2-k_\rho^2}}k_\rho dk_\rho dr^3 \tag{13}$$

Using the Hanker Function's Add-up theorem

$$H_0^2(k_\rho\rho)=\sum_{n=0}^{\infty}H_n^2(k_\rho\rho)e^{jn\varphi}J_n(k\rho') \tag{14}$$

Subscribe the Equation (14) into Equation (13)

$$U(k,\varphi,z)=\sum_{n=0}^{\infty}H_n^2(k_\rho\rho)e^{jn\varphi}J_n(k\rho')\frac{j}{8\pi}\int_0^\infty\frac{e^{-j\sqrt{k^2-k_\rho^2}(z-z')}}{\sqrt{k^2-k_\rho^2}}k_\rho dk_\rho \tag{15}$$

Transform the Equation (15)'s Integration order and add up, one gets

$$U'(k,\varphi,z)=\sum_{n=0}^{\infty}H_n^2(k_\rho\rho)e^{jn\varphi}e^{j\sqrt{k^2-k_\rho^2}z}\int_0^\infty\frac{j}{8\pi}J_n(k\rho')\frac{e^{-j\sqrt{k^2-k_\rho^2}z'}}{\sqrt{k^2-k_\rho^2}}k_\rho dk_\rho \tag{16}$$

Set $S_0=\int_0^\infty\frac{j}{8\pi}J_n(k\rho')\frac{e^{-j\sqrt{k^2-k_\rho^2}z'}}{\sqrt{k^2-k_\rho^2}}k_\rho dk_\rho$, and connect with Equation (9), and the Equation (16) is simplified as

$$U(k,\varphi,z)=\sum_{n=0}^{\infty}H_n^2(k_\rho\rho)e^{jn\varphi}e^{jk_z z}S_0 \tag{17}$$

Conduct 2D Fourier Transform to Equation (17)

$$\int_{-\infty}^{\infty}e^{-jk_z z}dz\int_0^{2\pi}U'(k,z,\varphi)e^{-jn\varphi}d\varphi=\sum_{n=0}^{\infty}H_n^2(k_\rho\rho)S_0 \tag{18}$$

Tidy up Equation (18) and one gets

$$S_0=\sum_{n=0}^{\infty}\frac{\int_{-\infty}^{\infty}e^{-jk_z z}dz\int_0^{2\pi}U'(k,z,\varphi)e^{-jn\varphi}d\varphi}{H_n^2(k_\rho\rho)} \tag{19}$$

When the distance between antenna and target satisfy the far field condition, and the following calculation approximation stands

$$\left|r-r'\right|\cong r-r\cdot r' \tag{20}$$

And

$$\frac{e^{-j2k|\mathbf{r}-\mathbf{r}'|}}{4\pi\left|r-r'\right|}=\frac{e^{-j2kr}}{4\pi\rho}e^{j2kr\cdot r'} \tag{21}$$

At the same time, the Hanker Function large volume approximation is

$$\underset{k_\rho\rho\to\infty}{H_n^{(2)}(k_\rho\rho)}=\sqrt{\frac{2}{\pi k_\rho\rho}}e^{-j\left(k_\rho\rho-\frac{2n+1}{4}\pi\right)} \tag{22}$$

Subscribe the Equations (19), (21), (22) into Equation (17), the transform relation between near field and far field scattering under cylinder scan mode after tidy-up

$$S_{FF}(k,\varphi,k_z)=\sqrt{\frac{\rho}{\pi k_\rho}}e^{-j\rho(k_\rho-k)}e^{j\frac{2n+1}{4}}\sum_{n=0}^{N}\frac{e^{jn\varphi}}{H_n^2(k_\rho\rho)}\int_{-\infty}^{\infty}e^{-jk_z z}dz\int_0^{2\pi}U'(k,z,\varphi)e^{-jn\varphi}d\varphi \tag{23}$$

The above equation is the near-far field transform relation under scan-frequency system, and it could be applied into the spot-frequency system, which needs only substitute $U(k,z,\varphi)$ with $u(k,z,\varphi)$, where the H_n^2 is the second sort n order Hanker Function, truncated at the $kD+10$ order, where D is the minimum diameter of the cylinder surrounding target which have the same concentric point with the survey circular. The $S_{FF}(k,\varphi,k_z)$ in Equation (23) is the 3-dimension wave number data of the target. Utilizing the 3D-IFFT imaging arithmetic under rectangular coordinate, conducting the 3D reverse Fourier transform to the Equation (23), one could get the far field image of the target. However, before conducting the 3D reverse Fourier transform, the extrapolated far field $S_{FF}(k,\varphi,k_z)$ needs to be interposed according to the relation $(k,\varphi,k_z) \rightarrow (k_x,k_y,k_z)$, in order to finish the reestablishment of the target image. Meanwhile, interpose the $S_{FF}(k,\varphi,k_z)$ according to the mapping relation of Equation (9), the far-field RCS is related to the far-field pattern via

$$\sigma(k,\phi) = 4\pi \left|S_{FF}(k,\phi)\right|^2 \tag{24}$$

3. SIMULATION EXAMPLES

In order to testify our transformation method, numerical simulation is conducted to observe the actual imaging performance. In the numerical scene, the point target's position and RCS amplitude is shown in Fig. 3. The simulation measurement parameters are: central frequency f_0 is 4 GHz, the scan band width B is 4 GHz, he frequency points number is 301, the cylinder scan radius is 5 m, the moving scale along axis z is ± 3 m, the scan step is 2 cm, the scan azimuth angle is $-180^\circ \sim 180^\circ$, the angle interval is 0.5°. The RCS variation relation with azimuth angle, pitch angle and frequency is shown in Figs. 4∼6.

Through calculation, the average square error of the near field extrapolation data and far field data in azimuth angle, pitch angle and frequency domain are 0.1608 dB (5° smooth window), 0.3046 dB (1° smooth window), 0.4101 dB. The 3-dimensional rebuild image is shown in Fig. 7. From the imaging results, one can find that the scattering center position in 3D image is identical

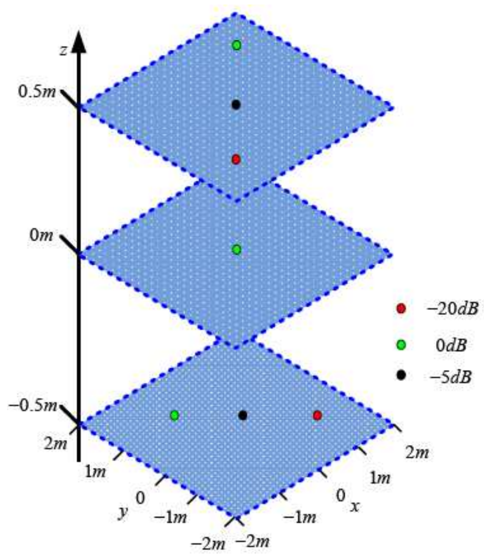

Figure 3: Scatters distribution map.

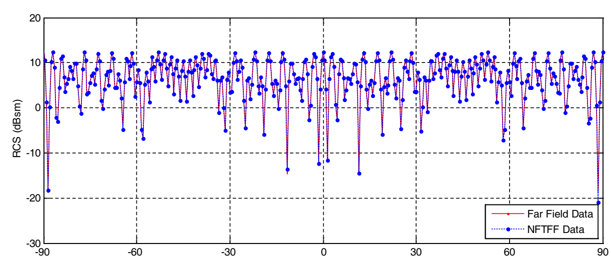

Figure 4: RCS variation with the azimuth.

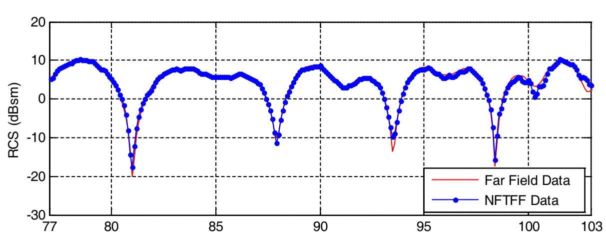

Figure 5: RCS variation with the pitch angle.

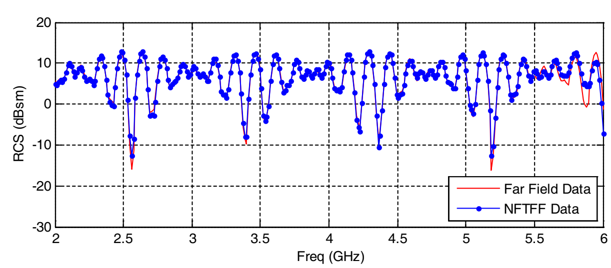

Figure 6: RCS variation with frequency.

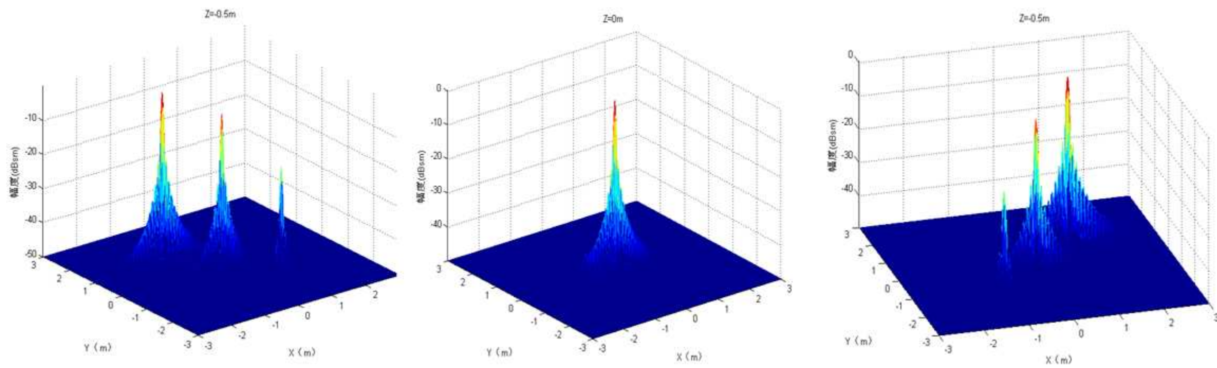

Figure 7: Point scatters 3D rebuild image.

with actual situation. And the largest position error is only 1 cm; the largest amplitude error of the scattering center is below 0.3 dB.

4. CONCLUSIONS

This article studied near field to far field transformation based on cylindrical scan mode. This arithmetic first transformed the double-distance spherical wave factor in echo data into the single-distance spherical wave factor, and utilize the 3D rectangular coordinate extension theorem of the spherical electro-magnetic wave into plan wave, established the relationship between near field backscatter and far field backscatter field, finally obtained the far field RCS character by 3D IFFT and 2D interpose and target's image. The numerical simulation result testified the validity and effectiveness of the above transformation arithmetic.

REFERENCES

1. Watkins, J. R., "Utilizing near-field measurements to characterize far-field radar signatures," Master Thesis, 2004.
2. Cady, E. M., "A study of near field data transformed to the far field for a canonical PEC scatter," Master Thesis, 2006.
3. LaHaie, I. J., "Overview of an image-based technique for predicting far field radar cross-section from near field measurements," *IEEE Ant. Prop. Mag.*, Vol. 45, No. 6, 159–169, 2003.
4. LaHaie, I. J., et al., "An improved version of the circular near field-to-far field transformation (CNFFFT)," *Proc. AMTA'05*, 196–201, 2005.
5. Norton, S. J. and M. Linzer, "Ultrasonic reflectivity imaging in three dimensions exact inverse scattering solutions for plane, cylindrical and spherical apertures," *IEEE Transactions on Biomedical Engineering*, 202–220, 1981.
6. Gao, C., Z. H. Xiao, and C. Ning, "Near-field three dimensional imaging and RCS extrapolation," *Antenna Journal B*, Vol. 2, 249–262, 2010.
7. Fischer, B. E., et al., "On the use of wavenumber migration for linear SAR image formation and near-field to far-field RCS transformation," *Proc. of 23rd Annual Meeting of the Antenna Measurement Techniques Association (AMTA'01)*, 117–122, Denver, CO, 2001.
8. LeBaron, E. I. and K. R. Aberegg, "Application of an image-based near field-to-far field transformation to measured data," *Proc. of the 19th Annual Meeting of the Antenna Measurement Techniques Association (AMTA'97)*, 340–345, Boston, MA, 1997.
9. Lopez-Sanchez, J. M. and J. Fortuny-Guasch, "3-D Radar imaging using range migration techniques," *IEEE Trans. Antennas Propagat.*, Vol. 48, 728–737, May 2000.
10. Hansen, J. E., *Spherical Near-field Antenna Measurements*, Peter Peregrinus Ltd., Stevenage, U.K., 1988
11. Fortuny-Guasch, J. and J. M. Lopez-Sanchez, "Extension of the 3-D range migration algorithm to cylindrical and spherical scanning geometries," *IEEE Trans.*, Vol. 49, No. 10, Oct. 2001.